Full-Duplex Millimeter-wave Radio over Fiber with 24 Gbps 4-QAM Downstream Signal in W-Band (75-110GHz)

Nauman Ashraf, Furqan Shaukat, Gulistan Raja and Ahmad Khalil Khan

***Abstract* — We propose a millimeter-wave radio over fiber transmission system in the W-band (75–110 GHz) with quadrature amplitude modulation and wavelength reuse ability. Optical millimeter-wave carriers are generated at the central station by frequency quadrupling a 16.75GHz local oscillator using two LiNb Mach-Zehnder modulators. 24 Gbps of downlink data is single side band modulated with one of the tones generated by LiNb Mach-Zehnder modulators and sent over a 30 km long single mode fiber. At the base station, beating of tones occurs at a high speed photodetector and generates an 87GHz millimeter wave containing the downlink data. Another local oscillator millimeter wave at 67GHz is generated with the use of fiber Bragg reflectors. This millimeter wave is used to down convert the uplink data received wirelessly from the user station to 4 GHz. The down converted uplink data is double side band modulated with the second tone which was received from the base station and partially reflected by fiber Bragg reflector and sent to the central station, thus keeping the access units simple. The simulation analysis for 4 and 16 quadrature amplitude modulation shows that the full duplex model has good performance with bit error rate below forward error correction limits even after 30 km standard single mode fiber transmission at 24 Gbps without any inline dispersion compensation.**

***Index Terms* — Bragg gratings; Frequency quadrupling; Millimeter wave communication; Radio over Fiber (RoF) technology; Wavelength reuse**

I. INTRODUCTION

Tremendous growth in the wireless applications, number of users, video approaching two-thirds of the world's mobile data traffic [1][2]. The emergence of bandwidth intensive applications such as 4k Ultra High Definition TV (UHDTV) demands the wireless transmission to support tens of gigabit per second of data rates. Despite of other benefits of wireless networks, they have limitations of lower offered data rates in contrast to the order of Gbps offered by the optical fibers [3][4][5].

Integration of fiber optics with wireless networks, Radio over Fiber technology (RoF), has attracted much attention by offering high data rate, wide bandwidth, mobility and low losses [6][7]. Wavelength reuse concept on an RoF system has been utilized in [8] but the model requires additional lightwave sources at both the central station and base stations. In an RoF system, a photonic millimeter wave (mm-wave) is generated at the central station (CS) and data is transmitted to remote antenna units (RAUs) on optical fiber [9][10]. A wavelength reuse technique through FBG was proposed in [11] utilizing phase modulation and stimulated Brillouin scattering effect with transmission up to 5Gbps. However, higher data rates can either be achieved by increasing the wireless spectral efficiency or by raising the carrier frequency up to the mm-wave range (30 to 300GHz). M-ary quadrature amplitude modulation (m-QAM) offers high levels of spectral efficiency and more tolerance to fiber dispersive parameters when optical mm-wave signal is traversed along a dispersive single mode fiber (SMF) [12]. Much higher orders of modulation come at cost of receiver complexity and an increased electrical signal to noise ratio (SNR) requirements that lead to complex and expensive RAUs. On the other hand, the impacts of fiber chromatic dispersion, a major challenge, results in every spectral component experiencing unlike phase shifts [13]. These shifts depend on the fiber-link distance, fiber-dispersion parameter and modulation frequency. This results in rotation of each constellation point around the origin in quadrature amplitude modulated electrical signals. Modulation of both the carriers in the millimeter wave with a dual drive MZM was proposed in [14] but this adds complexity to each base station as they will require a setup of local oscillator for uplink optical signal generation.

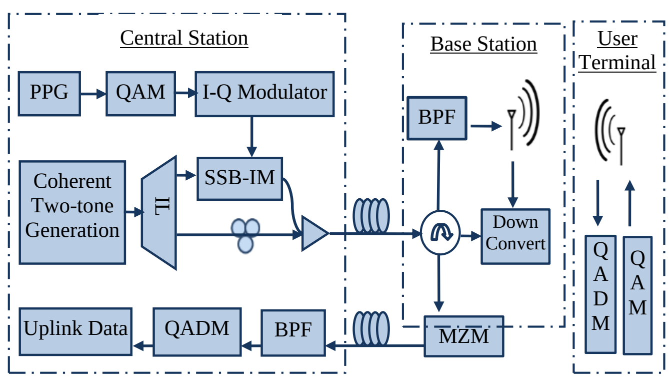

Fig. 1 Block Diagram of the Radio over Fiber System. PRBG, pseudo random bit sequence generator; IL, interleaver Demux; QADM, quadrature amplitude demodulator; BPF, band pass filter.

Nowadays, mm-wave RoF research focuses the V-band (50–75 GHz) containing the 7GHz unlicensed band at 60GHz and licensed bands at 66-75GHz. The 35GHz W-band at 75-110GHz is also being researched for very high data rates due to the available wide bandwidth [15]. Moreover, the W-band also offers minimal atmospheric attenuation compared to the 60GHz band.

Nauman Ashraf is with the Department of Electrical Engineering, University of Engineering and Technology (UET) Taxila, Pakistan. Furqan Shaukat is with the Department of Electronics Engineering UET Taxila, Sub-campus Chakwal Pakistan. Gulistan Raja is with the Department of Electronics Engineering UET Taxila, Pakistan. Ahmad Khalil Khan is with the Department of Electrical Engineering UET, Taxila, Pakistan. Email:nauman091@hotmail.com,furqan415@hotmail.com, ahmad.khalil @uettaxila.edu.pk, gulistan.raja@uettaxila.edu.pk, Manuscript received on Feb 24,2017 revised on March 19,2017 and accepted on May 15,2017.

 ISSN – 1999-4974

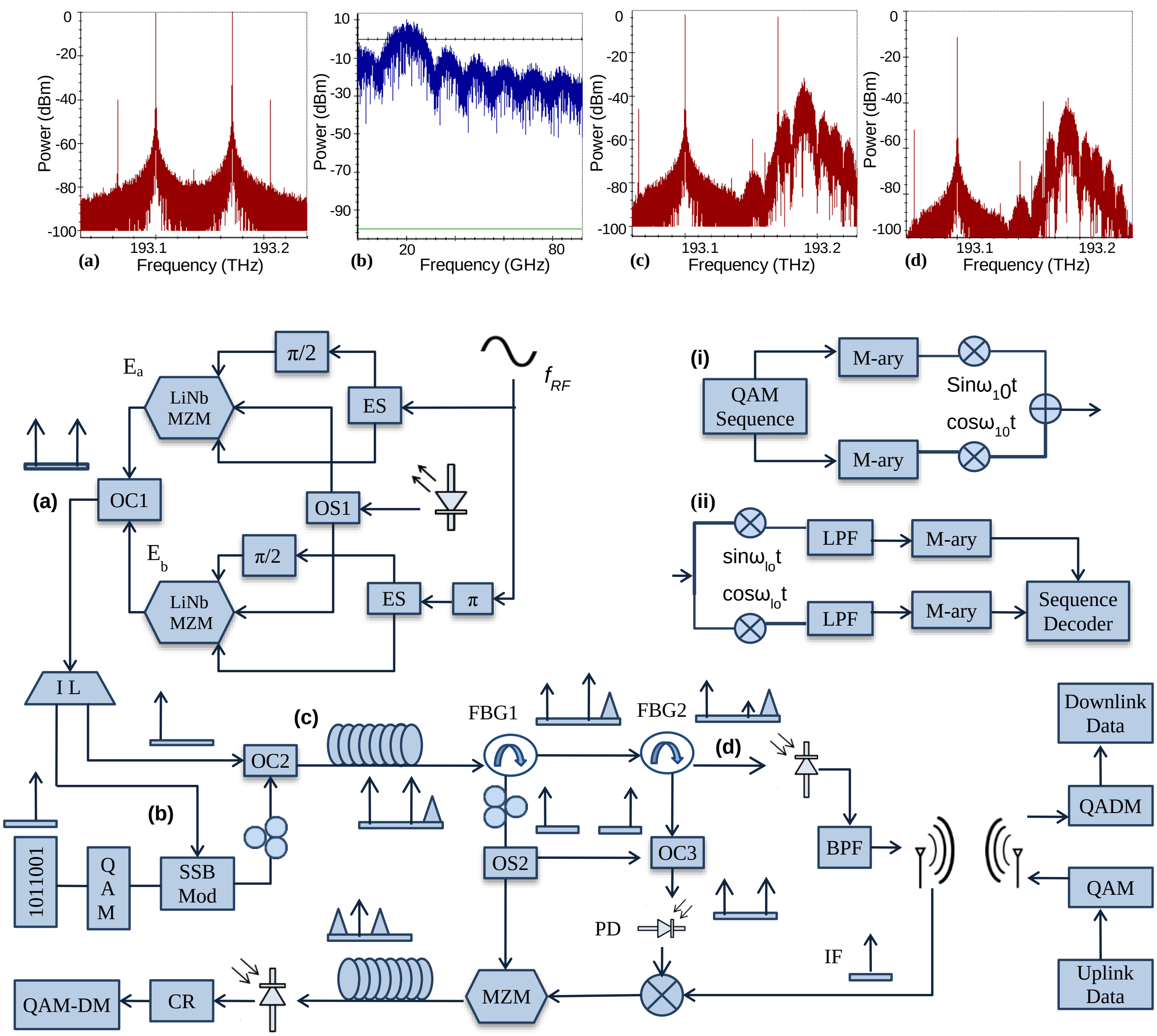

Fig. 2 Simulation model and radio frequency (RF) spectrums of the proposed Radio over Fiber System. (a) millimeter-wave generation by frequency quadrupling. (b) QAM 20GHz downstream electrical signal. (c) Modulated lightwave signal transmitted over optical fiber. (d) Downlink optical signal after carrier tone reflection by FBG2. (i) Quadrature amplitude modulator. (ii) Quadrature amplitude Demodulator. FBG, Fiber Bragg gratings. OC, optical coupler; MZM, Mach-Zehnder modulator; ES, Electrical Splitter; LPF, low pass filter; LD, laser diode; PD, photodetector; CR, clock recovery.

Therefore, an RoF system supporting both of the V-band and W-Band is a promising solution for gigabit services [16]. In this work, a full duplex mm-wave RoF system in the W-band with wavelength reuse capability in the V-Band band is proposed and modeled. The block diagram is shown in Fig. 1. Performance of the system is analyzed for a 30 km long SMF carrying 4-QAM and 16-QAM vector modulated signals for data rates up to 24Gbps and 16Gbps respectively.

At the central station, mm-wave is generated with a single laser source by frequency quadrupling a 16.75GHz local oscillator. One of the two carrier tones of the mm-wave, after separation with a WDM interleaver Demux, is single sideband (SSB) modulated with downlink data and coupled with the unchanged second tone. The light wave after polarization control is fed into a dispersive SMF for downlink transmission to the base station. At the base station two mm-waves, at 87GHz and 67GHz, are generated for downlink transmission and down conversion of the uplink data with the use of FBG reflectors and beating at high speed photodiode. FBG reflector also reflects a portion of power in the unmodulated carrier from the downlink that will be used for uplink electrical signal modulation. The uplink data received wirelessly from the user station at 71GHz is down converted to 4GHz, double sideband (DSB) modulated to keep the base station simple and fed into a 30km long SMF for uplink transmission. The performance of the downlink and uplink channel is then analyzed mathematically. The proposed model is little affected by fiber chromatic dispersion because of the SSB modulation. Moreover, single carrier modulation keeps the system simple compared to the complexity of OFDM modules. Uplink lightwave source is centralized at the central station. External local oscillators for uplink down conversion, dispersion compensation unit or DSP units for constellation equalization at the RAU are not required.

This paper is organized as follows. Section II describes the operating principle of the proposed model followed by the simulation results and conclusion in sections III and IV respectively.

II. OPERATING PRINCIPLE

The numerical model of the proposed full-duplex W-band RoF system is shown in the Fig. 2. Lightwave, expressed as $E_1 e^{j\omega_1 t}$, is generated with a single laser diode emitting a continuous lightwave of amplitude E_1 and angular frequency $\omega_1 = 2\pi f_1$. The light wave is power split with an optical splitter and fed into two parallel LiNb Mach-Zehnder Modulators. Radio frequency electrical signals $V_{RF}\cos(\omega_{RF}t)$ and $V_{RF}\cos(\omega_{RF}t+\pi/2)$ are applied to the two arms of the first modulator, whereas the signal is given an electrical phase shift of 180° before being applied to the second modulator as shown in the Fig. 2. The outputs of the modulators E_α and E_b are given in (1) and (2) respectively.

$$E_a = \frac{E_1}{4} e^{j\omega_1 t}\left[e^{jm\cos\left(\omega_{RF}t+\frac{\pi}{2}\right)} + e^{jm\cos(\omega_{RF}t)} e^{j\pi\frac{V_{dc}}{V_\pi}} \right] \quad (1)$$

$$E_b = \frac{E_1}{4} e^{j\omega_1 t}\left[e^{jm\cos\left(\omega_{RF}t+\frac{3\pi}{2}\right)} + e^{-jm\cos(\omega_{RF}t)} e^{j\pi\frac{V_{dc}}{V_\pi}} \right] \quad (2)$$

Where, m is the modulation index of the modulator expressed as $\pi V_{RF}/V_\pi$. Outputs E_a and E_b are coupled and lightwave is now comprised of negative and positive second-order sidebands. The output is expressed in (3) [17],

$$E_c(0,t) = E_1 \sum_{n=-\infty}^{\infty}\left[J_n(m) \times \sin\left(\frac{n\pi}{4}\right) \times \cos\left(\frac{n\pi}{2}\right) \times e^{(j(\omega_0+n\omega_{RF})t+\frac{n\pi}{4})}\right] \quad (3)$$

Here, $J_n(m)$ is the nth-order Bessel function of the first kind. Equation (3) shows that the sidebands of nth-order are all suppressed, except for n = 4k-2, where k represents an integer.

The second order sidebands of the generated mm-wave, at $\omega_1 + 2\omega_{RF}$ and $\omega_1 - 2\omega_{RF}$, are separated with a WDM interleaver Demux to obtain the two carriers. One of the carriers at $\omega_1 + 2\omega_{RF}$ is SSB modulated with the electrical M-QAM intermediate frequency (IF) signal containing the downlink data. This is done with a Dual-drive Mach-Zehnder Modulators (DDMZM). The other tone at $\omega_1 - 2\omega_{RF}$ remains unmodulated and is coupled with the modulated tone after polarization control. Lightwave, containing the downlink data is comprised of tones at $\omega_1 - 2\omega_{RF}$ and $\omega_1 + 2\omega_{RF} + \omega_{IF}$) which is now transmitted over SMF towards the base station.

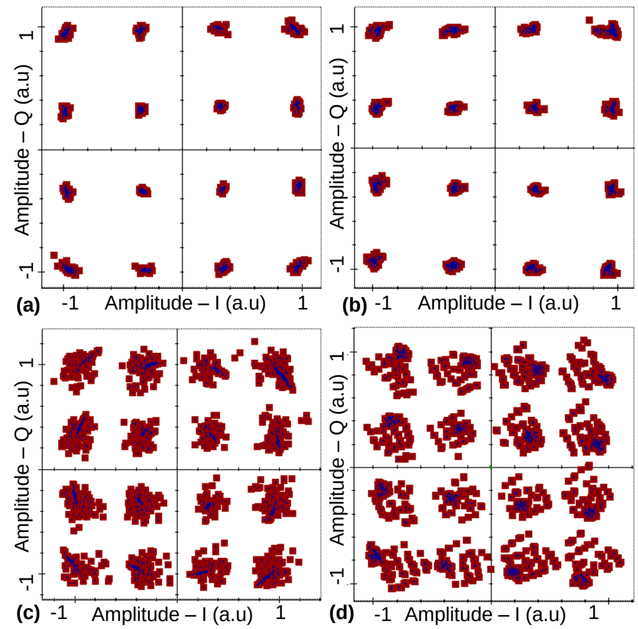

Fig. 3 16-QAM downlink electrical signal constellation diagrams. (a) 12Gbps transmitted. (b) 16Gbps transmitted. (c) 12Gbps received. (d) 16Gbps received.

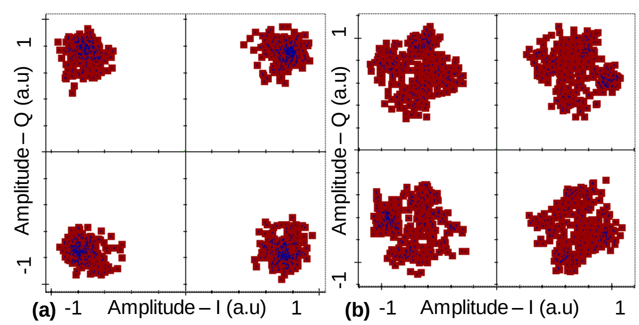

Fig. 4 4-QAM downlink electrical signal constellation diagrams. (a) 24Gbps transmitted. (b) Received after 30km.

At the base station, part of the carrier tone at $\omega_1 - 2\omega_{RF}$ is reflected with the help of a narrow-band Fiber Bragg grating (FBG1) with 60% reflectivity in combination with an optical circulator. This reflected tone is power split into two carriers by another optical splitter (OS2). One of the carriers will be used for modulation with the uplink data. Another Bragg grating (FBG2) at frequency $\omega_1 + 2\omega_{RF}$ is used to reflect most of the carrier from the downlink data.

At the base station, a high speed photodiode detects the optical signal transmitted by the base station 30 km away. Here, beating of tones takes place generating an electrical mm-wave signal in the W-band centered at 87GHz. Now the received Photodiode current comprises of a beat component, a constant DC component and a high frequency component.

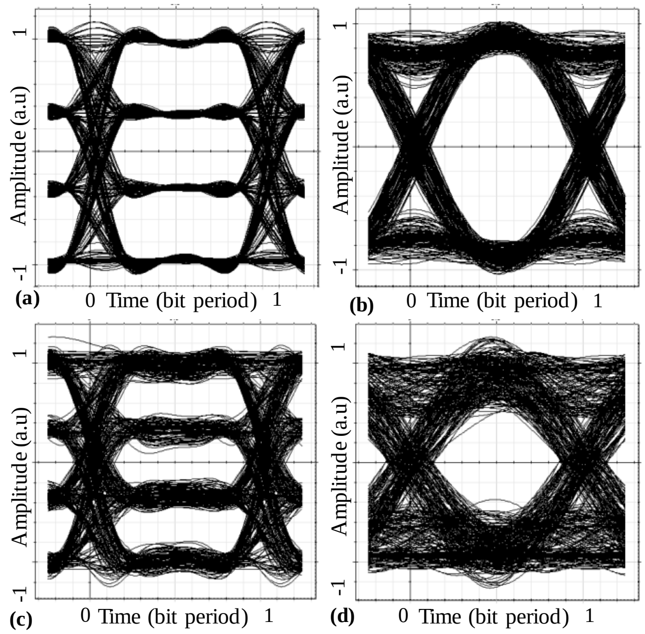

Fig. 5 Downlink Eye diagrams. (a) 16-QAM transmitted at 16Gbps. (b) 4-QAM transmitted at 24Gbps. (c) Received 16-QAM. (d) Received 4-QAM.

We are interested in the mm-wave generated at frequency $4\omega_{RF} + \omega_{IF}$, which is filtered out and transmitted wirelessly to the user station. We down convert this mm-wave signal to the baseband frequency to analyze transmission performance.

The uplink data at frequency ω_{UP} is simultaneously received in the 66-75GHz band from the user station by the RAU. The uplink data also needs to be down converted to an intermediate frequency. For this purpose, an optical coupler (OC3) couples the reflected tones from the two FBGs. A second photodiode at the base station detects these tones $\omega_1 \pm 2\omega_{RF}$. The process of beating there generates another mm-wave at $4\omega_{RF}$. This mm-wave is used as a local oscillator to down convert the uplink data received from the user station. After down conversion to intermediate frequency, the uplink data is double side band modulated with the carrier reflected by FBG1 at $\omega_1 - 2\omega_{RF}$. Uplink data is sent over SMF towards the central station. Double side band modulation keeps the simplicity of the base station.

III. Simulation Results and Discussions

The simulation setup is developed in the OptiSystem software platform and the results are analyzed in MATLAB. We have simulated the model for 4-QAM and 16-QAM digital modulation techniques with data rates up to 24-Gbps and 16Gbps respectively. Optical signal generation at downlink shown in Fig. 2 is performed by using a single CW laser source at a central frequency of 193.1335THz. The two LiNb Mach-Zehnder Modulator with half wave voltage 4V and 25dB extinction ratio are driven by a single 16.75GHz local electrical oscillator with a phase shift of 180^{o} for the second modulator.

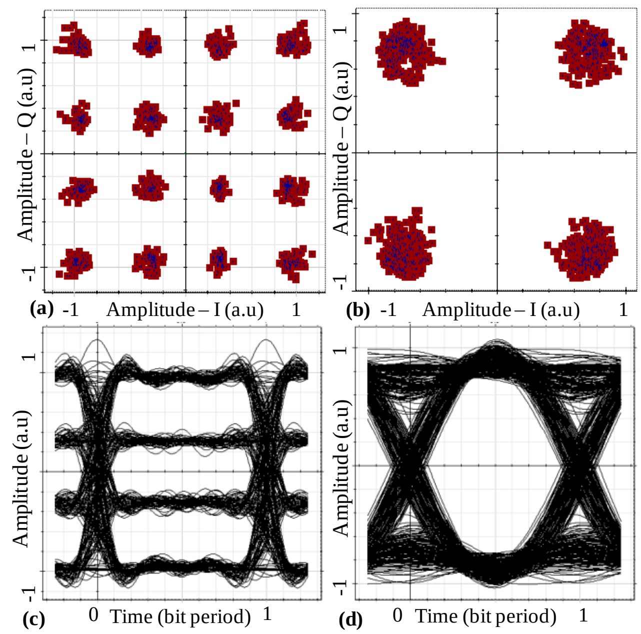

Fig. 6 Uplink received electrical signal constellations and eye diagrams.

The output of the coupler (OC1) is a frequency quadrupled mm-wave with carriers at 193.1THz and 193.167THz having 67GHz spacing. The generated mm-wave is separated into two tones by a WDM interleaver Demux. Now, the modulated data is coupled with the unmodulated tone using an optical coupler.

A polarization controller is employed to control the polarization of the lightwave. The obtained lightwave is transmitted to the base stations over single mode fiber of length up to 30km with chromatic dispersion value of 16ps/nm/km, power attenuation of 0.2dB/km and differential group delay of 0.15 ps/sqrt(km) and an effective core area of 80µm^2. At the base station, part of the carrier tone at 193.1THz is reflected with a narrow-band Fiber Bragg grating (FBG1) in combination with an optical circulator. This FBG has a 60% reflectivity. The reflected tone is power split into two carriers by an optical splitter. Another Bragg grating (FBG2) at frequency 193.167 and reflectivity up to 96% is used to reflect most of the carrier from the downlink data.

A photodiode with responsivity of 1A/W detects lightwave signal and beating occurs to generate an electrical mm-wave signal centered at 87GHz. We coherently demodulate the signal with a 20GHz local oscillator to analyze the performance of the system. In real scenario, it will be wirelessly transmitted to the user stations. A second photodiode at the base station detects the reflected and coupled tones from the two FBGs at 193.10 THz and 193.67THz. It generate a 67GHz local oscillator signal to down convert the uplink data received from the user station at 71GHz. After down conversion to intermediate frequency, the uplink data is double side band modulated with the FBG reflected 193.1GHz carrier. Uplink data is transmitted over a SMF of 30km length with chromatic dispersion of 16.75ps/nm/km, power attenuation of 0.2dB/km, differential group delay of 0.15ps/sqrt(km) and an effective core area of 80µm^2. At the central station, the uplink data is demodulated and the performance of system is analysed.

The performance of the downlink and uplink optical system is analysed mathematically for different fiber lengths, received power and data rates on the basis of Bit error rate (BER), error vector magnitude (EVM) and modulation error ratio (MER). All the received constellation diagrams are first normalized with respect to the transmitted symbols. Fig. 3 shows the transmitted and received constellation diagrams of the in-phase and quadrature 16-QAM modulated electrical signals for downlink data. The constellation diagrams of the 4-QAM electrical signal sent at 24-Gbps are given in Fig. 4. Fig. 5 displays the eye diagrams of quadrature components of the downlink electrical signals. The constellations and eye diagrams of quadrature components in the 5-Gbps uplink signal are shown in Fig. 6. Mathematical results have been graphically represented in Fig. 7-11. It can be seen from the constellation and eye diagrams that for back to back cases, points are separated by a very good distance although some noise due to the photodiodes and electrical components can be observed.

Constellation diagrams of 16-Gbps and 12-Gbps of 16-QAM along with 24-Gbps of 4-QAM modulated data electrical signals are shown in Fig. 3 and Fig. 4 for BTB case and 30km of optical transmission. In case of 4-QAM, constellation points do not overlap each other as seen in Fig. 4. This results in good eye openings as shown in Fig. 5(b) and 5(d). Similarly, for 16-QAM modulated data at 12-Gbps, system shows good performance and constellation points remain separated even after 30km of fiber transmission. In the case of 16-QAM modulated data, constellation points start to overlap as fiber length is increased from 30km and results in narrower eye opening.

Uplink data which was modulated by the reflected carrier received from the central station shows good results as well and the constellation points remain separated for 5-Gbps of M-QAM modulated data even after more than 30km of dispersive fiber without any inline dispersion compensation technique applied. The rotations caused by the fiber chromatic dispersion are equalized and no forward error correction (FEC) technique has been used.

Like BER, error vector magnitude and modulation error ratio are two useful tools for the prediction of scheme's dynamic performance. EVM and MER are used to assess the performance of vector signals [18][19]. They can be calculated from the received constellations with respect to the transmitted symbols. The constellations are first normalized. The relation for EVM is expressed as in (4),

$$\mathrm{EVM} = \frac{\left[\sqrt{\sum_{n=1}^{N}\left(|\hat{I}_n-\alpha_I I_n|^2+|\hat{Q}_n-\alpha_Q Q_n|^2\right)}\right]}{\left[\sqrt{\sum_{n=1}^{N}\left(|\alpha_I I_n|^2+|\alpha_Q Q_n|^2\right)}\right]} \qquad (4)$$

Where, I_n and Q_n are the in-phase and quadrature measurements of the nth symbol in the transmitted burst. At the receiver, $\hat{I}_n$ and $\hat{Q}_n$ measurements are received which are normalized by the normalization factors α_I and α_Q.

On the other hand, MER (dB), which quantifies the performance of digital Radio, is calculated as the ratio of the RMS reference power vector to that of the error vector's power. This is given in (5).

$$\mathrm{MER(dB)} = \frac{\left[10\log_{10}\left[\sqrt{\sum_{n=1}^{N}\left(|\alpha_I I_n|^2+|\alpha_Q Q_n|^2\right)}\right]\right]}{\left[\sqrt{\sum_{n=1}^{N}\left(|\hat{I}_n-\alpha_I I_n|^2+|\hat{Q}_n-\alpha_Q Q_n|^2\right)}\right]} \qquad (5)$$

In-phase and quadrature measurements of the transmitted symbols are given by I_n , Q_n, whereas the received in-phase and quadrature measurements are represented in (5) as $\hat{I}_n$ and $\hat{Q}_n$. Whereas α represents the normalization factor for the constellations.

BER for the M-QAM constellations is estimated from the EVM by the relation given in (6) [20].

$$\mathrm{BER} = \left[\frac{\left(1-\mathrm{M}^{-\frac{1}{2}}\right)}{(\log_2 \mathrm{M})}\right]\mathrm{erfc}\sqrt{\frac{\frac{3}{2}}{(\mathrm{M}-1)\times \mathrm{EVM}^2}} \qquad (6)$$

Relationship between the log of BER and percentage EVM is graphically represented in Fig. 7 which depicts that higher orders of M-QAM are more prone to noise.

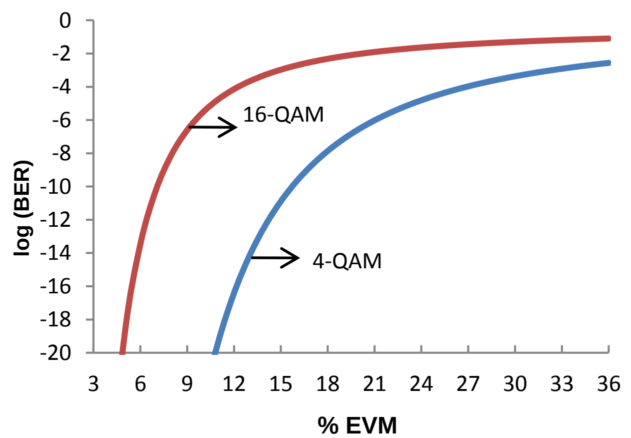

Fig. 7 Relationship between BER and EVM for m-QAM electrical signals

The curve in Fig. 8 shows the change in EVM with respect to the increase in optical fiber length for different data rates. As the fiber length starts to increase, dispersion parameters and attenuation degrade the transmitted optical signal resulting in the overlapping of the constellation points at the receiver. This in turn causes the increase in the power of error vector. This effect can be observed with the increase in magnitude of the error vector as the fiber length increases as shown in the Fig. 8.

 ISSN – 1999-4974

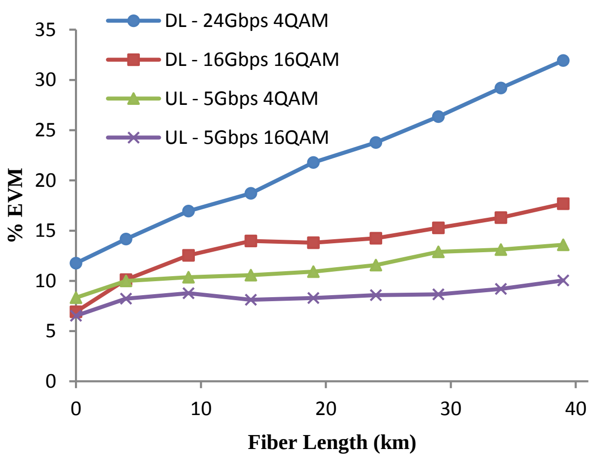

Fig. 8 EVM vs. optical fiber length for downlink and uplink transmission

At received optical power greater than 10dBm, the constellation points of the received signal scatter further because of the fiber nonlinearities which are prominent at higher optical powers. These effects result in higher EVM values which are also seen when not enough optical power is received and the receiver's noise parameters cannot be overcome. This variation in the calculated EVM values with the changing received optical power can be observed for both the uplink and downlink transmission in in Fig. 9 and Fig. 10 respectively. The data rate for uplink transmission is lower than downlink transmission which results in lower overall error vector magnitude values.

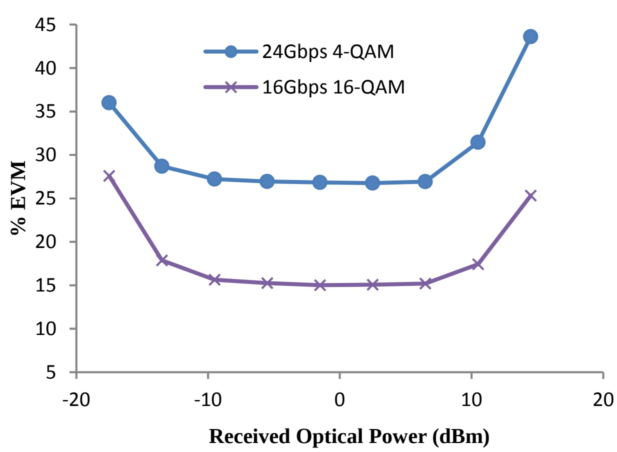

Fig. 9 EVM vs received optical power for downlink transmission.

MER plots for 16 and 4-QAM modulation techniques are shown in Fig. 11. Higher MER values depict better transmission performance. With fiber dispersion coming into effect at greater fiber lengths, the constellation points in the received signal start to overlap resulting in the increase of error vector's power which in turn decreases the modulation error ratio as depicted in Fig. 11.

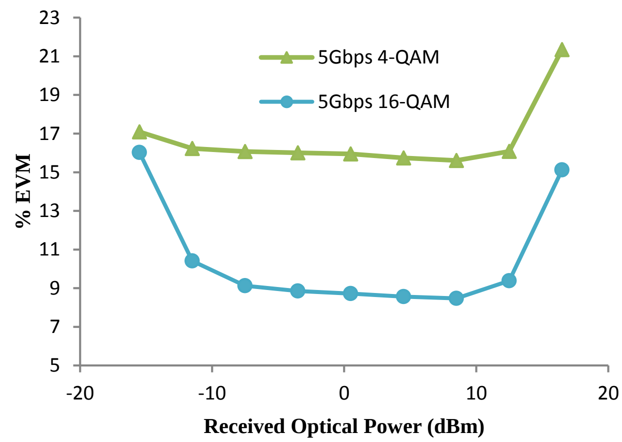

Fig. 10 EVM vs. received optical power for uplink transmission.

At 24-Gbps of 4-QAM transmission over a 30km optical fiber, EVM of 27% (BER ≅ $1x10^{-4}$) is achieved when the received optical power is -2dBm. It reduces to 21.8% (BER ≅ $2.1x10^{-6}$) for 20Gbps data rate. For 30km transmission at 12-Gbps and 16-Gbps of 16-QAM modulated data, EVM of 12.22% (BER ≅ $1x10^{-4}$) and 14.9% (BER ≅ $1x10^{-3}$) is reported with the proposed technique. Whereas, EVM of 14.1% at 10-Gbps data rate and received optical power of 2dbm was reported in [12].

With the proposed model, the improvements in the achieved BER values for downlink transmission are given in Table I. BER values are given for the received optical power of -2dBm with fiber nonlinear effects included. For all the cases, BER remains below the FEC limit of BER = $2x10^{-3}$. Similarly uplink shows fairly good performance with bit error rates of approximately $1x10^{-7}$ and $2x10^{-10}$ for 5-Gbps of 16 and 4-QAM transmission. BER values of $4.8x10^{-4}$ and $2x10^{-8}$ are obtained after down conversion and 30km transmission of 7.5-Gbps of 16-QAM and 4-QAM electrical signals and BER values way below the FEC limit. It can be observed from the plots in Fig. 9 and Fig. 10 that system shows good performance for a wide range of received optical powers.

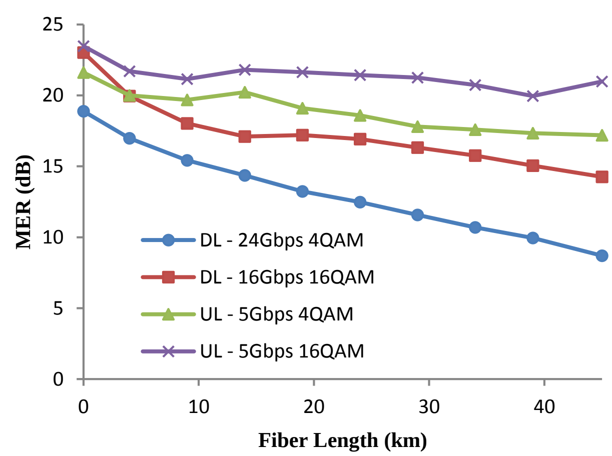

Fig. 11 Modulation error ratio vs. optical fiber length for downlink and uplink transmission.

 ISSN – 1999-4974

At high input laser powers, fiber nonlinear effects become more dominant and the performance degrades and results in higher EVM values, whereas at low received powers, EVM again becomes larger because of the low optical signal to noise ratio.

TABLE I. COMPARISON OF TECHNIQUES

	Achieved Data Rates		Fiber Length(km)		BER (FEC Limit = $2x10^{-3}$)		
	16-QAM	4-QAM	10 Gbps	24 Gbps	10Gbps 16-QAM	16Gbps 16-QAM	24Gbps 4-QAM
Ma et al. 2012 [12].	10	-	30	-	$5.6x10^{-4}$	-	-
Proposed Model.	16	24	60	30	$1.3x10^{-4}$	$1x10^{-3}$	$1x10^{-4}$

IV. CONCLUSION

In this paper we have proposed a full-duplex RoF system in the W-Band with wavelength reuse capability while maintaining the simplicity of RAUs. Millimeter wave is generated at the central station by frequency quadrupling using a single laser source only. Downlink data is single side band modulated and lightwave signal overcomes fiber chromatic dispersion effectively. BER for 24-GBps of 4-QAM data measured after more than 30km of optical transmission remains below the FEC limit of BER = $2x10^{-3}$ at a good range of received optical power. At 24-Gbps of 4-QAM transmission over a 30km optical fiber BER ≅ $1x10^{-4}$ is achieved for the received optical power of -2dBm. For 16-QAM transmission at 16-Gbps, BER ≅ $1.2x10^{-3}$ is achieved. At the base station, FBG not only reflects the desired power in the reserve carrier for uplink data modulation but it is also useful in the generation of a local oscillator electrical signal by a photodiode to down convert the uplink signal to intermediate frequency thus keeping the RAU simple.

REFERENCES

[1] R. Zhang, J. Ma, W. Liu, W. Zhou, and Y. Yang, "A multi-band access radio-over-fiber link with SSB optical millimeter-wave signals based on optical carrier suppression modulation," Opt. Switch. Netw., vol. 18, pp. 235–241, 2015.

[2] C. V. N. I. Forecast, "Cisco visual networking index: Global mobile data traffic forecast update 2009-2014," Cisco Public Information, Febr., vol. 9, pp. 2015–2020, 2010.

[3] V. A. Thomas, M. El-Hajjar, and L. Hanzo, "Millimeter-wave radio over fiber optical upconversion techniques relying on link nonlinearity," IEEE Commun. Surv. Tutorials, vol. 18, no. 1, pp. 29–53, 2016.

[4] A. M. Zin, M. S. Bongsu, S. M. Idrus, and N. Zulkifli, "An overview of radio-over-fiber network technology," in 2010 International Conference on Photonics, ICP2010, 2010.

[5] R. Herschel and C. G. Schaffer, "Radio-over-fiber systems for next generation wireless access," in 2011 International Students and Young Scientists Workshop "Photonics and Microsystems", STYSW 2011, 2011, pp. 54–58.

[6] Wenjing Xu et al., "High spectral purity millimeter wave generation and wavelength reuse radio over fiber system based on modified double sideband," in 2016 25th Wireless and Optical Communication Conference (WOCC), 2016, pp. 1–4.

[7] G. Cheng, B. Guo, S. Liu, and W. Fang, "A novel full-duplex radio-over-fiber system based on dual octupling-frequency for 82 GHz W-band radio frequency and wavelength reuse for uplink connection," Optik (Stuttg)., vol. 125, no. 15, pp. 4072–4076, 2014.

[8] L. Nadeem and R. Asif, "FSK signal generation with wavelength reuse capability in 8 Gbit/s radio over fiber systems," Front. Optoelectron., vol. 6, no. 3, pp. 303–311, 2013.

[9] J. Ma and Y. Li, "A full-duplex multiband access radio-over-fiber link with frequency multiplying millimeter-wave generation and wavelength reuse for upstream signal," Opt. Commun., vol. 334, pp. 22–26, 2015.

[10] A. Mumtaz and M. K. Islam, "Next generation multi-service access gateway for Radio over Fiber wireless systems," in 2011 7th International Conference on Emerging Technologies, ICET 2011, 2011.

[11] R. K. Al-Dabbagh and H. S. Al-Raweshidy, "64-GHz millimeter-wave photonic generation with a feasible radio over fiber system," Opt. Engineering, vol. 56, no. 2, 2017.

[12] J. Ma, Y. Zhan, M. Zhou, and H. Liang, "Full-duplex radio over fiber with a centralized optical source for a 60 GHz millimeter-wave system with a 10 Gb/s 16-QAM downstream signal based on frequency," J. Opt., 2012.

[13] V. Sharma, A. Singh, and A. K. Sharma, "Challenges to radio over fiber (RoF) technology and its mitigation schemes - A review," Optik (Stuttg)., vol. 123, no. 4, pp. 338–342, 2012.

[14] T. Yang et al., "A novel radio-over-fiber system with dual millimeter-wave signals generated simultaneously," Optik., vol. 127, no. 16, pp. 6532-6540, 2016.

[15] X. Pang et al., "25 Gbit/s QPSK hybrid fiber-wireless transmission in the W-band (75-110 GHz) with remote antenna unit for in-building wireless networks," IEEE Photonics J., vol. 4, no. 3, pp. 691–698, 2012.

[16] L. Cheng, C. Liu, Z. Dong, J. Wang, M. Zhu, and G. K. Chang, "Real-time dual-band wireless videos in millimeter-wave radio-over-fiber system," Opt. Fiber Technol., vol. 19, no. 6 PART A, pp. 529–532, 2013.

[17] N. Al-Shareefi et al., "Development of a new approach for high-quality quadrupling frequency optical millimeter-wave signal generation without optical filter," Prog. Electromagn. Res., vol. 134, 2013.

[18] W. Freude et al., "Quality metrics for optical signals: Eye diagram, Q-factor, OSNR, EVM and BER," in International Conference on Transparent Optical Networks, 2012.

[19] A. O. Aldhaibani, S. Yaakob, R. Q. Shaddad, S. M. Idrus, M. Z. Abdul Kadir, and A. B. Mohammad, "2.5 Gb/s hybrid WDM/TDM PON using radio over fiber technique," Optik (Stuttg)., vol. 124, no. 18, pp. 3678–3681, 2013.

[20] H. A. Mahmoud and H. Arslan, "Error vector magnitude to SNR conversion for nondata-aided receivers," IEEE Trans. Wirel. Commun., vol. 8, no. 5, pp. 2694–2704, 2009.

 ISSN – 1999-4974

APPENDIX

A. *Millimeter Wave Generation*

From (1), the output of the first LiNb Mach-Zehnder modulator E_a can be simplified using the Euler's identity where V_π is the switching voltage and $V_{dc} = 0$, we get the relation given in (7).

$$E_a = \frac{E_1}{4} e^{j\omega_1 t}\left[e^{jm\cos\left(\omega_{RF}t+\frac{\pi}{2}\right)} - e^{jm\cos(\omega_{RF}t)}\right] \quad (7)$$

By applying the Jacobi-Anger expansion to (4) we get

$$E_a = \frac{E_1}{4} e^{j\omega_1 t}\left[\sum_{n=-\infty}^{\infty} j^n J_n(m)\ e^{jn\left(\omega_{RF}t+\frac{\pi}{2}\right)} - \sum_{n=-\infty}^{\infty} j^n J_n(m)\ e^{jn(\omega_{RF}t)}\right]$$

$$E_a = \frac{E_1}{4} e^{j\omega_1 t}\left[\sum_{n=-\infty}^{\infty} J_n(m)\ e^{j(n\omega_{RF}t+n\pi)} - \sum_{n=-\infty}^{\infty} J_n(m)\ e^{j(\omega_{RF}t+n\frac{\pi}{2})}\right]$$

$$E_a = \frac{E_1}{4} e^{j\omega_1 t}\left[\sum_{n=-\infty}^{\infty} J_n(m)\ e^{j(n\omega_{RF}t+\frac{3n\pi}{4}+\frac{n\pi}{4})} - \sum_{n=-\infty}^{\infty} J_n(m)\ e^{j(\omega_{RF}t+\frac{3n\pi}{4}-\frac{n\pi}{4})}\right]$$

$$E_a = \frac{E_1}{4} e^{j\omega_1 t}\left[\sum_{n=-\infty}^{\infty} J_n(m)\ e^{j\left(n\omega_{RF}t+3n\frac{\pi}{4}\right)}\left(e^{j\left(n\frac{\pi}{4}\right)} - e^{-j\left(n\frac{\pi}{4}\right)}\right)\right]$$

$$E_a = \frac{E_1}{2}\left[\sum_{n=-\infty}^{\infty} J_n(m)\ \sin\left(\frac{n\pi}{4}\right) e^{j((\omega_1 t+n\omega_{RF})t+3n\frac{\pi}{4})}\right] \quad (8)$$

Here J_n is the nth order Bessel function of first kind. We can get the equation for the optical wave from the second modulator using the same procedure,

$$E_b = \frac{E_1}{2}\left[\sum_{n=-\infty}^{\infty} J_n(m)\ \sin\left(\frac{n\pi}{4}\right) e^{j\left((\omega_1+n\omega_{RF})t-n\frac{\pi}{4}\right)}\right] \quad (9)$$

Coupling the outputs of two modulators Ea and Eb from (8) and (9), we get the lightwave E_c which is now comprised of negative and positive second-order sidebands in (10),

$$E_c = \frac{E_1}{2}\left[\sum_{n=-\infty}^{\infty} J_n(m)\ \sin\left(\frac{n\pi}{4}\right) e^{j\left((\omega_1+n\omega_{RF})t+3n\frac{\pi}{4}\right)} + \sum_{n=-\infty}^{\infty} J_n(m)\ \sin\left(\frac{n\pi}{4}\right) e^{j\left((\omega_1+n\omega_{RF})t-n\frac{\pi}{4}\right)}\right] \quad (10)$$

$$E_c = \frac{E_1}{2}\left[\sum_{n=-\infty}^{\infty} J_n(m)\ \sin\left(\frac{n\pi}{4}\right) e^{j\left((\omega_1+n\omega_{RF})t+n\frac{\pi}{2}+n\frac{\pi}{4}\right)} + \sum_{n=-\infty}^{\infty} J_n(m)\ \sin\left(\frac{n\pi}{4}\right) e^{j\left((\omega_1+n\omega_{RF})t-n\frac{\pi}{2}+n\frac{\pi}{4}\right)}\right]$$

$$E_c = E_1 e^{j\omega_1 t}\left[\sum_{n=-\infty}^{\infty} J_n(m)\, e^{j\left((\omega_1+n\omega_{RF})t+n\frac{\pi}{4}\right)}\left\{e^{jn\frac{\pi}{2}} - e^{-jn\frac{\pi}{2}}\right\}\right]$$

$$E_c = \sum_{n=-\infty}^{\infty} J_n(m)\ \sin\left(\frac{n\pi}{4}\right)\cos\left(\frac{n\pi}{2}\right)\exp\left[j(\omega_1 + n\omega_{RF})t + \frac{n\pi}{4}\right] \quad (11)$$

Which is same as (3) showing that there is constructive interference for nth order sidebands for value (4k-2). The reason for this is the phase shift of π given to the local oscillator signal before being fed into the second LiNb Mach-Zehnder modulator.

 ISSN – 1999-4974